ELSEVIER

Journal of Hazardous Materials 42 (1995) 87–102

JOURNAL OF HAZARDOUS MATERIALS

Characterization of chromium doped tricalcium silicate using SEM/EDS, XRD and FTIR

O.E. Omotoso[a], D.G. Ivey[a,*], R. Mikula[b]

[a] *Department of Mining, Metallurgical and Petroleum Engineering, University of Alberta, Edmonton, Alta., Canada T6G 2G6*

[b] *CANMET Western Research Centre, Devon, Alta., Canada TOC 1E0*

Received 29 November 1994: accepted 20 January 1995

Abstract

The containment of chromium in tricalcium silicate (C_3S[1]) has been investigated. Tricalcium silicate is a major component in ordinary Portland cement (OPC), and chromium compounds used as dopants simulate chromium wastes that might be stabilized in a cement matrix. Scanning electron microscopy (SEM) and energy dispersive X-ray spectroscopy (EDS) were used to probe the distribution of chromium in the stabilized waste form and also to identify the microstructural changes in the normal hydration products of C_3S accompanying the addition of chromium as Cr(III) and Cr(VI). X-ray diffraction (XRD) was used to monitor the hydration reaction of C_3S and formation of crystalline calcium hydroxide (CH). The effect of chromium addition on the condensation of the orthosilicate units in C_3S was followed with Fourier transform infrared spectroscopy (FTIR). Standard acetic acid leaching tests were carried out to evaluate the mobility of chromium in the Cr(III)/C_3S and Cr(VI)/C_3S systems. Probable mechanisms of chromium containment in the amorphous calcium silicate hydrate (C–S–H) phase are discussed.

1. Introduction

Hazardous wastes that are not eliminated by incineration or reclamation are usually stabilized and solidified in a suitable binder before disposal in landfills. The most common binder for containing heavy metal wastes is an ordinary Portland cement (OPC)/pozzolana matrix. Depending on the heavy metal ion, the mode of containment ranges from chemical fixation to physical encapsulation to produce a stable cement/waste solid matrix. Stability is defined by the amount of heavy metal leached under standard conditions. Understanding the containment mechanisms and

* Corresponding author.

[1] Cement Notations: C = CaO; S = SiO_2; H = H_2O; CH = $Ca(OH)_2$.

SSDI 0304-3894(95)00012-7

leaching behaviour has been impeded because of the complexity of cement chemistry and the coupled cement/waste chemistry. In an attempt to simplify the complex OPC system, tricalcium silicate (C_3S or alite) is often used to model the hydration of Portland cement. C_3S is the major constituent of OPC clinker, representing 40–55% by weight of the total amount. The main reaction product of C_3S and β-dicalcium silicate (C_2S), or belite (another major component of cement clinker), is amorphous calcium silicate hydrate (C–S–H) which is responsible for the strength and stability of cement. Typically, the main silicate species in the pore solution of hydrating C_3S are $H_3SiO_4^-$ and $H_2SiO_4^{2-}$ [1]. As the pH increases, linear polymers are formed from the monomeric silicate anions [2, 3].

Understanding the stabilization and solidification mechanisms of hazardous metals in cement requires the use of different characterization techniques. Each method has limitations that restrict a comprehensive understanding of the hazardous waste/cement systems. Among the various techniques that are being used to study stabilization/solidification processes in cement, electron microscopy (SEM, TEM) coupled with energy dispersive X-ray spectroscopy (EDS) provides microstructural and morphological information as well as the spatial distribution of the hazardous metal in the cement matrix. Fourier transform infrared spectroscopy (FTIR), X-ray photoelectron spectroscopy (XPS) and ^{29}Si nuclear magnetic resonance (NMR) could be used to probe the molecular structure of the amorphous C–S–H.

Chromium stabilization in cement/alite has been investigated by several authors [4–8]. When added in the soluble hexavalent form, Cr is leached from the chromium waste/cement matrix by standard leaching solutions [4, 5]. Bishop et al. [5] observed that the concentration of Cr in the leachate increases with increasing surface area of the cement/Cr waste matrix. This was attributed to the greater ion exchange capacity of smaller particles. Cr(III) solutions, on the other hand, are better contained and more leach resistant in cement matrices than Cr(VI). Leaching and electron microscopic studies of the Cr(III)/alite systems [6] indicate that Cr is located in all the hydration products of cement. In addition, Cr(III) appears to increase the Ca/Si ratio in the C–S–H phases, suggesting that Cr may be substituting for Si. The charge deficiency is balanced by cations present as impurities in alite. FTIR studies [7] show that Cr(III) affects the silicate tetrahedral vibrational modes, lending credence to the possibility of Cr^{3+} substitution for Si^{4+}, with K^+ acting to compensate for charge deficiencies. ^{29}Si NMR studies of Cr(III)/OPC 28 day old paste [8] indicate that Cr(III) retarded the polymerization of the orthosilicate units, since no polymeric silicate species were found.

This investigation aims at gaining an insight into the mode of chromium containment in portland cement by using C_3S, a less complex and major component of cement, and a combination of microstructural, microanalytical (SEM/EDS and XRD) and molecular (FTIR) characterization techniques. 1 *M* Cr solutions were used to enhance identification of the specific effects that Cr has on the hydration of C_3S. 0.1 *M* Cr solutions (typical of Cr concentration in heavy metal contaminated wastes) were initially employed, but neither SEM nor FTIR could detect the changes induced in the hydration products even though leaching studies indicated that Cr(III) was completely immoblized. The effects of varying Cr concentrations on the stabilization/solidification process are currently being investigated by the authors.

2. Materials and methods

The C_3S used in this study was produced by sintering stoichiometric ratios of reagent grade SiO_2 and $CaCO_3$ at 1600 °C for 24 h. This was ground with alumina balls to less than 5 μm and characterized with X-ray diffraction. Using the modified Franke extraction technique [9], the free CaO content was found to be less than 0.1%.

1 *M* Cr solutions were prepared from analytical reagent grade $Cr(NO_3)_3 \cdot 9H_2O$ (as Cr(III)) and CrO_3 (as Cr(VI)). The Cr solutions were separately mixed with C_3S (solution/C_3S weight ratio = 0.5) to make a paste. Distilled water/C_3S pastes were also made to serve as standards. The pastes were cast into plastic moulds and stored in humidifying chambers flushed with N_2 and plugged with ascarite to minimize carbonation of the reaction products. Curing under N_2 is essential because carbonation proceeds much faster in the small samples ($\approx$2 g) used in the laboratory than in the very large quantities of waste/cement containment systems encountered in practice. Samples were removed after 1, 31 and 60 days for analyses. The hydration reactions were stopped in the one day old samples by adding isopropanol and evacuating in a desiccator for 18 h. Samples for X-ray diffraction analysis and FTIR were ground in cyclohexane for about 2 h to a particle size of less than 2 μm. Samples for leaching experiments were crushed to about 50 μm using a mortar and pestle.

Leaching tests were carried out on the 60 day old samples using the EPA standard toxicity characteristic leaching procedure (TCLP) (acetic acid, pH 2.88) [10]. This entails leaching the sample for 18 h with constant agitation. This was further modified by renewing the leachant every 18 h to maintain a driving force for leaching and to observe the relationship (if any) between the leaching rates of the metal ions contained in the C–S–H phase. A Perkin-Elmer atomic absorption spectrometer (AAS) was used to analyze the acidified leachate for Ca, Cr and Si.

A Hitachi S-2700 scanning electron microscopy (SEM) with a Link eXL energy dispersive X-ray spectrometer (EDS) was used for microstructural and microanalytical characterization of the unleached samples. A Nicolet 750 Magna FTIR was used to obtain FTIR spectra. Potassium bromide pellets were used in the mid-infrared region (400–4000 cm^{-1}) and cesium iodide pellets used in the far-infrared region (50–600 cm^{-1}). The resolution of both spectra is 2 cm^{-1}. X-ray diffraction patterns were obtained with a Philips PW 1050/80 X-ray diffractometer, using Cu Kα radiation. Samples were packed in a hollow aluminium sample holder. Diffraction patterns were collected in triplicates to eliminate misinterpretation of the 0.49 nm CH (calcium hydroxide) peak, which is highly susceptible to preferred orientation despite the small particle size of the samples.

3. Results and discussions

3.1. Electron microscopy and X-ray diffraction studies

Fig. 1 shows an SEM micrograph and EDS spectrum of fibrous C–S–H obtained from the standard H_2O/C_3S paste after hydration for 24 h. Comparing the XRD

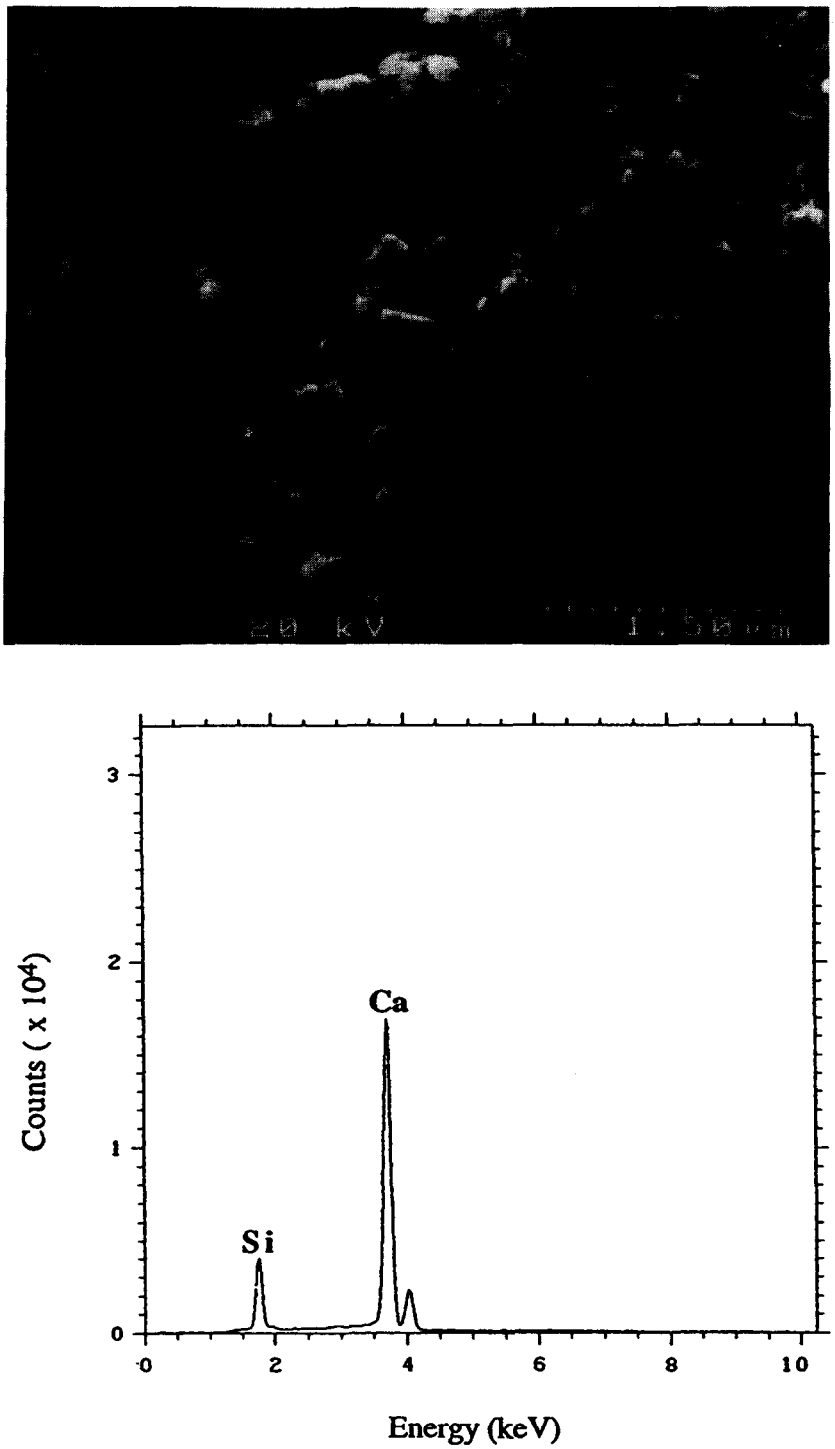

Fig. 1. SEM micrograph and EDS spectrum of one day old H_2O/C_3S paste showing fibrous C–S–H.

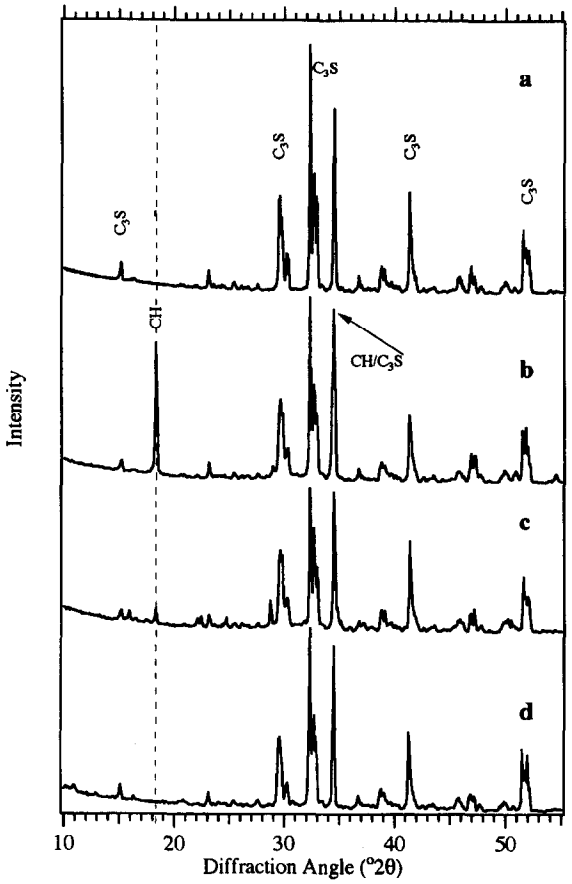

Fig. 2. XRD patterns of anhydrous C_3S and one day old pastes: (a) C_3S; (b) H_2O/C_3S; (c) 1 *M* Cr(VI)/C_3S, (d) 1 *M* Cr(III)/C_3S.

pattern of anhydrous C_3S (Fig. 2(a)) and that of the standard paste (Fig. 2(b)), it is apparent that a substantial amount of calcium hydroxide forms after one day. The matrix becomes denser with age as large crystals of calcium hydroxide form and fill the pores along with C–S–H fibres growing into the pores.

Addition of Cr(VI) does not have a significant effect on the microstructure. In the one day old samples, Cr was found in both the C–S–H and CH phases (Fig. 3). In an aqueous solution, CrO_3 is present as the oxyanion, $HCrO_4^-$, which deprotonates in an alkaline medium typical of hydrating C_3S, to give the chromate ion; CrO_4^{2-} [11]. The amount of CH formed in the Cr(VI) doped C_3S is reduced compared with the standard C_3S/H_2O mixture (XRD pattern in Fig. 2(c)). Additional peaks, not present in the standard occur at $2\theta = 16°$, 17.5° and 28.7°. These peaks are yet to be identified, but may be due to the formation of calcium chromate adsorbed on the CH and C–S–H phases. This possibility is currently being studied with the use of electron

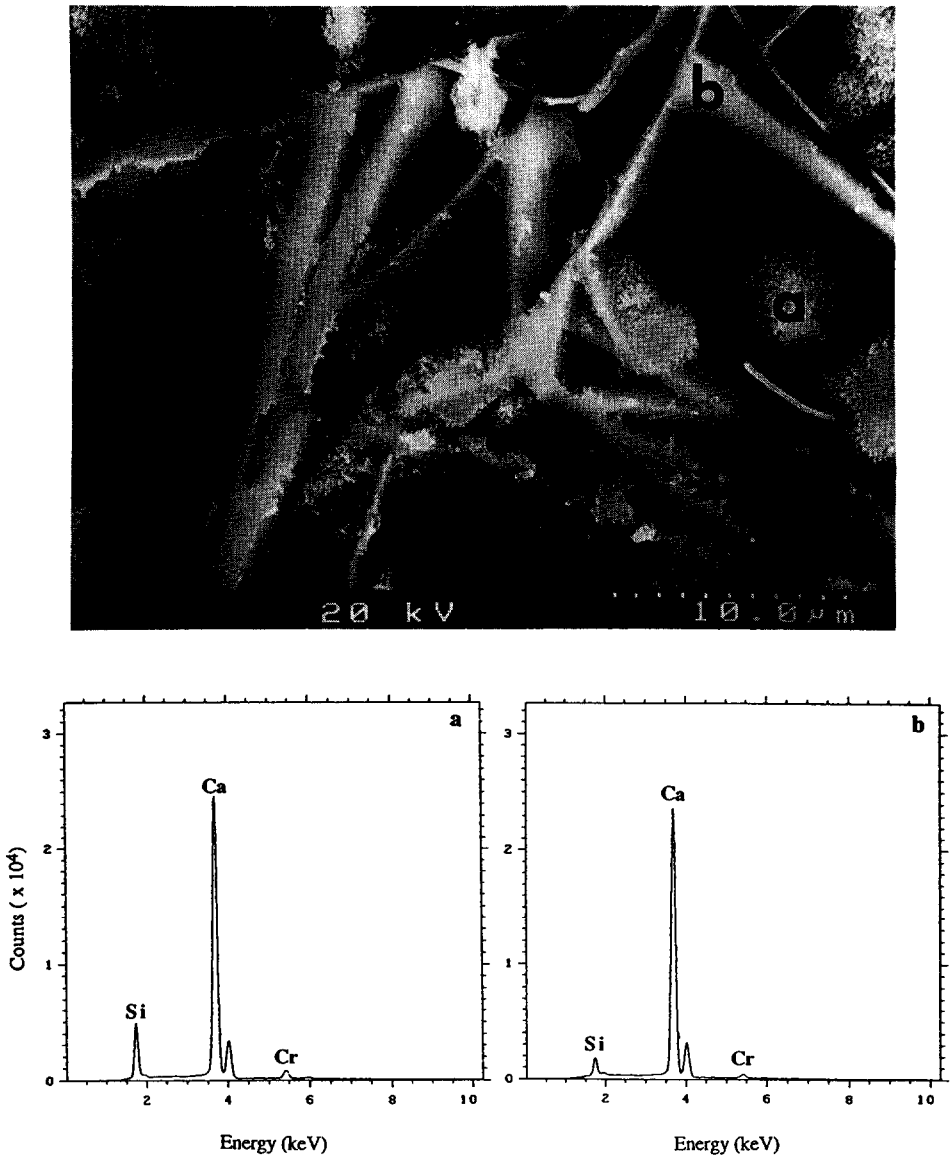

Fig. 3. SEM micrograph and EDS spectra of one day old Cr(VI)/C_3S paste. The region indicated by (a) is C–S–H while region (b) is calcium hydroxide.

diffraction techniques. The microstructure of the one day old, Cr(VI) doped C_3S (Fig. 3) persisted for the 31 and 60 day old samples.

Fig. 4 shows an SEM micrograph and EDS spectra of a one day old Cr(III)/C_3S paste. Cr is concentrated in the long rectangular rods. Transmission electron

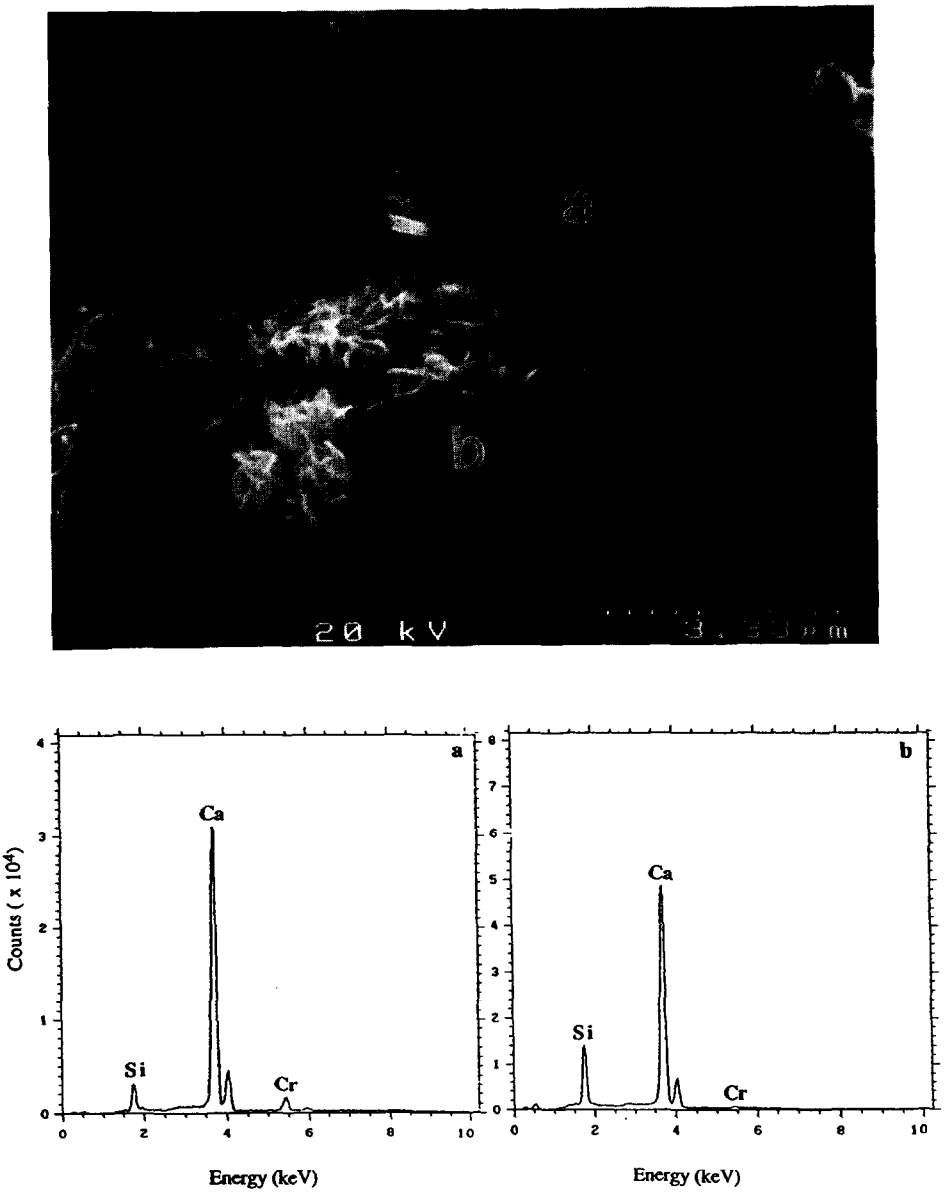

Fig. 4. SEM micrograph and EDS spectra of one day old Cr(III)/C_3S paste, showing (a) Cr-rich rods and (b) freshly emerging C–S–H.

microscopy and electron diffraction studies (not shown) reveal that the rods are amorphous with high concentrations of Ca and Cr but very little Si. The growth of fibrous C–S–H and calcium hydroxide (Fig. 2(d)) appears to be hindered, as significantly lower amounts of fibrous C–S–H and CH were detected relative to the

standard hydrated paste. After 31 days, XRD studies indicate that the consumption of C_3S and growth of calcium hydroxide are accelerated when compared with the C_3S/H_2O and Cr(VI) doped pastes (Fig. 5). The Cr-rich rods persisted after 31 days, with substantial amounts of Cr also found in the fibrous C–S–H areas (Fig. 6). After 60 days, the Cr-rich rods could not be found. Large crystals of Cr-free calcium hydroxide were identified as well as C–S–H areas containing significant amounts of Cr.

3.2. *FTIR spectroscopy*

The FTIR transmission spectrum for the C_3S used is shown in Fig. 7a. The main vibrations are: asymmetric stretching of the silicate tetrahedra (ν_3 SiO_4^{4-}) at 939 and 873 cm^{-1}; symmetric stretching (ν_1 SiO_4^{4-}) at 810 cm^{-1}; out-of-plane bending vibration (ν_4 SiO_4^{4-}) at 525 cm^{-1} and the in-plane bending vibration (ν_2 SiO_4^{4-})

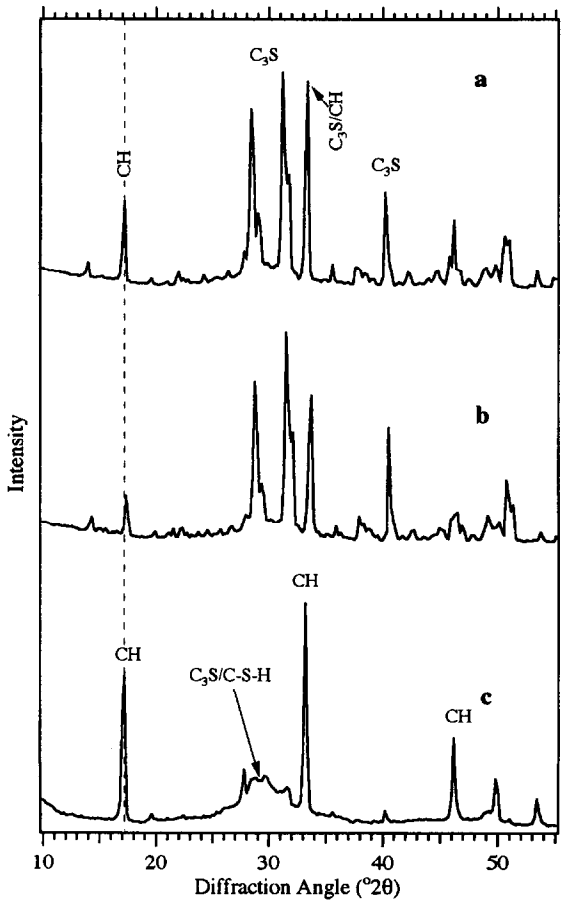

Fig. 5. XRD patterns of 31 day old pastes: (a) H_2O/C_3S; (b) 1 *M* Cr(VI)/C_3S; (c) 1 *M* Cr(III)/C_3S.

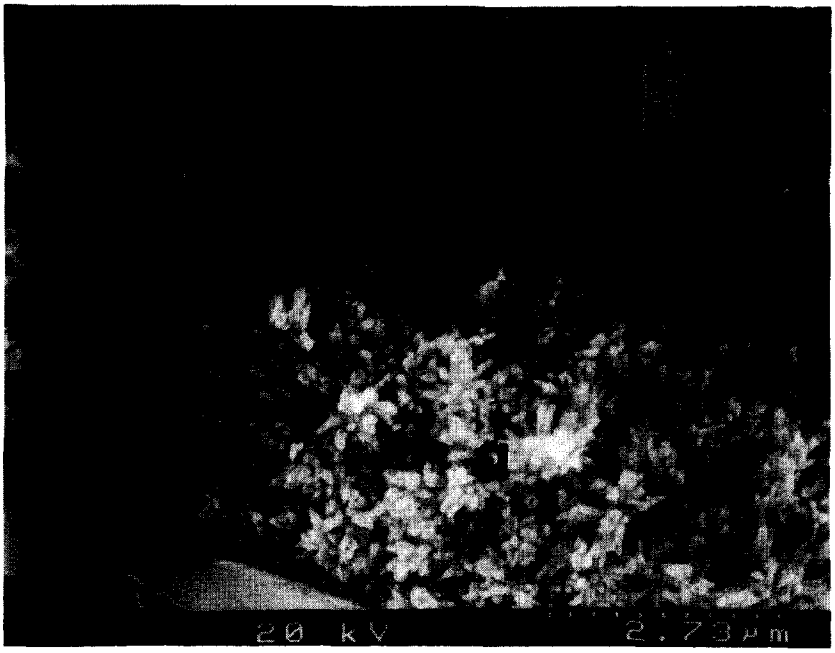

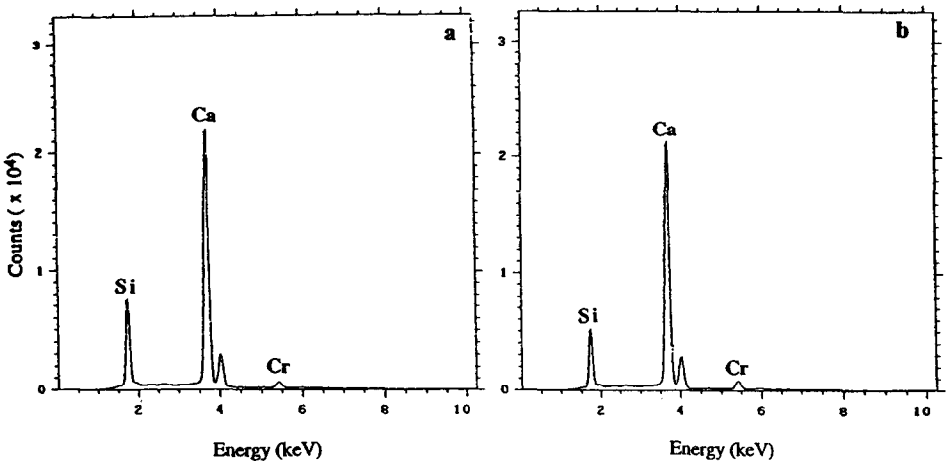

Fig. 6. SEM micrograph and EDS spectra of 31 day old Cr(III)/C_3S paste, showing (a) Cr-rich C–S–H and (b) Cr-rich rods.

centered around 452 cm^{-1}. These assignments are in agreement with previous studies [12–14]. Condensation of the silicate units along the C_3S trigonal axis causes the ν_3 SiO_4^{4-} to shift to higher wavenumbers. However, condensation hinders the bending vibrations, particularly the ν_4 SiO_4^{4-}, causing a shift to lower wave numbers. An

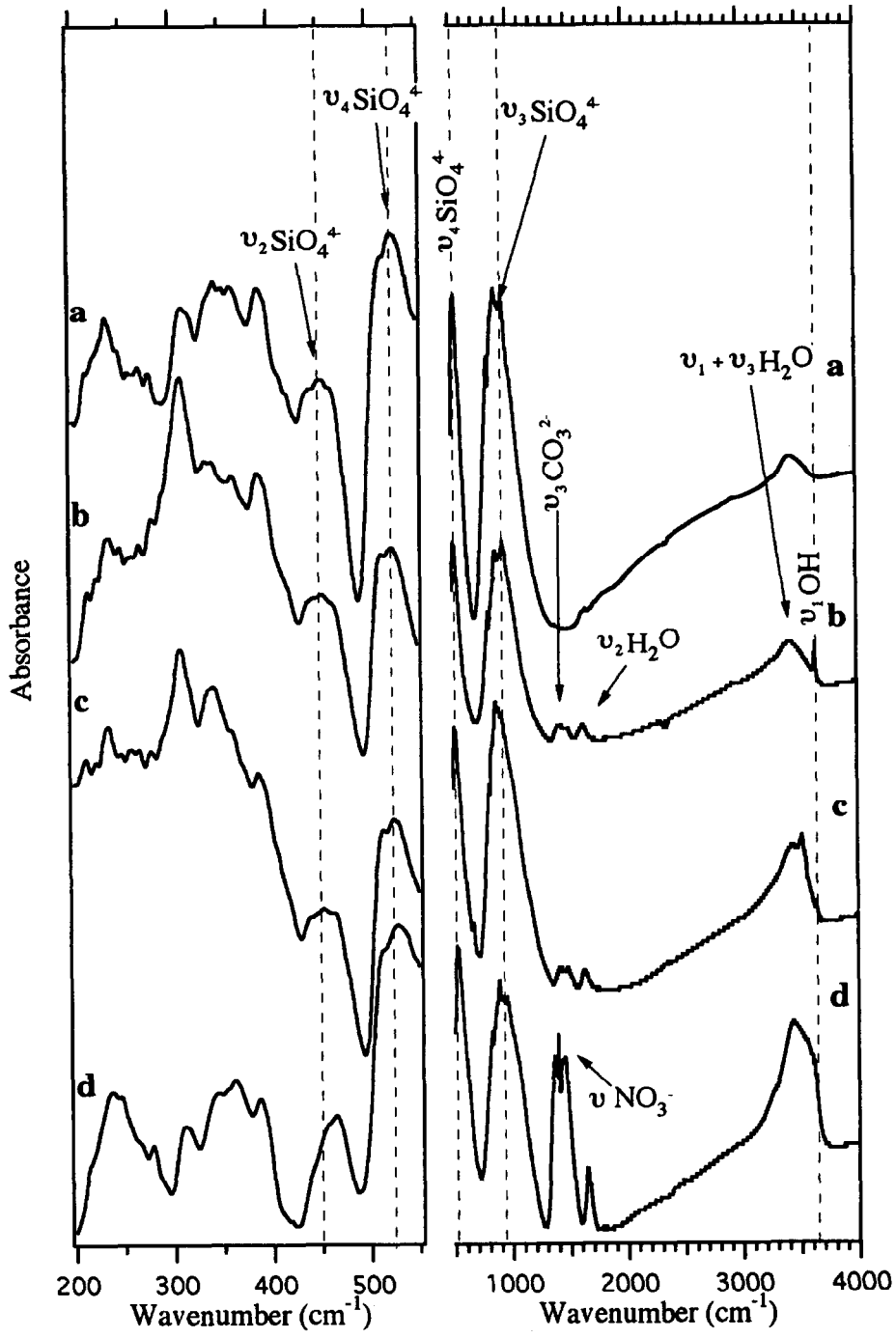

Fig. 7. FTIR (far-IR and mid-IR) of anhydrous C_3S and one day old pastes: (a) C_3S; (b) H_2O/C_3S; (c) 1 *M* Cr(VI)/C_3S; (d) 1 *M* Cr(III)/C_3S.

attendant reduction in the intensities of all the vibrational modes is expected as more C_3S is consumed. Fig. 7(b) shows the standard paste (H_2O/C_3S) hydrated for 24 h. The sharp band at 3644 cm^{-1} is due to the symmetric stretching ν_1 (OH) of $Ca(OH)_2$. The broad band around 3440 cm^{-1} is due to ν_3 and ν_1 (H_2O) and at 1630 cm^{-1}, the ν_2 (H_2O). These are lattice water vibrations [15]. Also the vibrational bands at 1420–1490 cm^{-1}, 870 cm^{-1} (coincides with one of the ν_3 SiO_4^{4-} vibrations) and 313 cm^{-1} are due to ν_3 CO_3^{2-}, ν_2 CO_3^{2-} and translatory lattice modes in calcite, respectively.

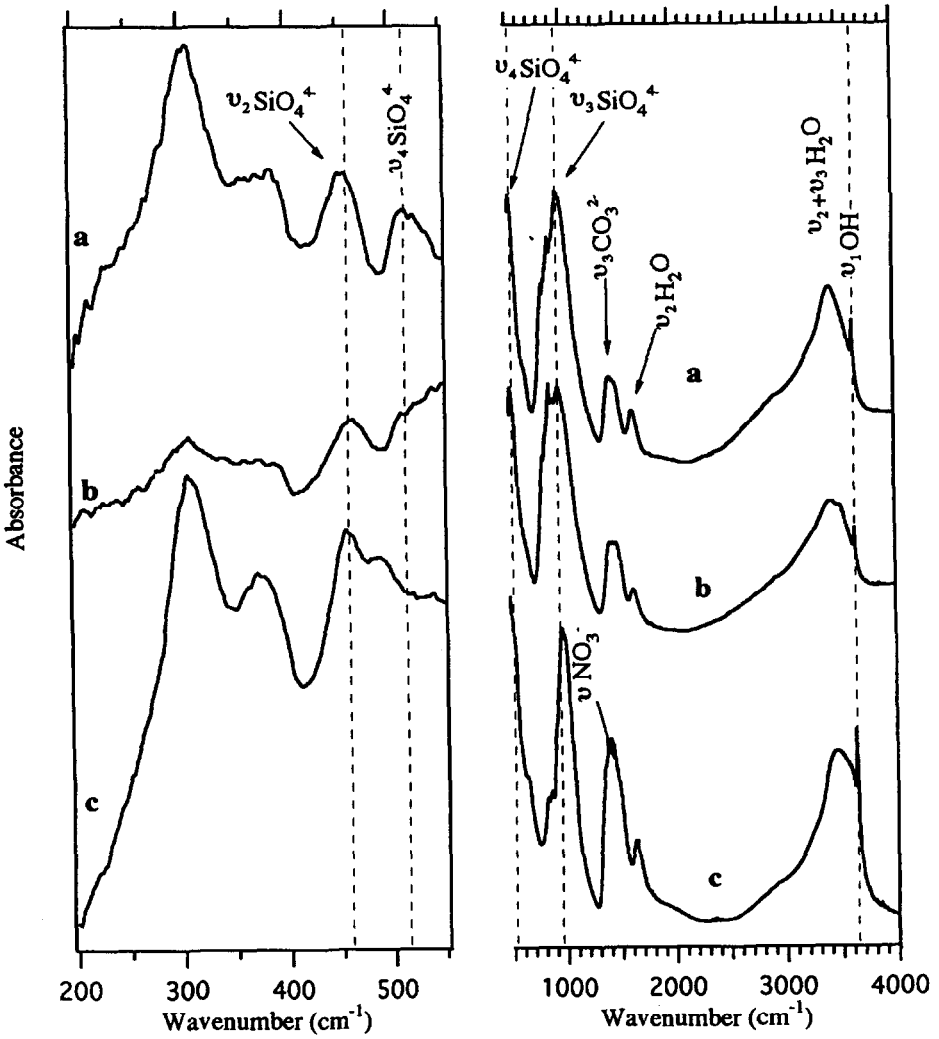

Fig. 8. FTIR (far-IR and mid-IR) of 60 day old pastes: (a) H_2O/C_3S; (b) 1 *M* Cr(VI)/C_3S; (c) 1 *M* Cr(III)/C_3S.

Table 1
FTIR (medium-IR and far-IR) spectra assignments of anhydrous and Cr-doped tricalcium silicate

Band assignment (cm^{-1})	C_3S	H_2O/C_3S		Cr(III)/C_3S		Cr(VI)/C_3	
		1 day	60 days	1 day	60 days	1 day	60 days
ν_2 (SiO_4^{4-})	453 s, b*	452 s, b	452 s, b	465 s, b	456 b	452 b	452 b
ν_4 (SiO_4^{4-})	525.5 vs	525 vs	514 b	525.5 vs	489 b	525.5 vs	513 b
ν_1 (SiO_4^{4-})	810 sh	811 sh	812 sh	811 sh	830 sh	812 sh	816 sh
ν_3 (SiO_4^{4-})	873 s	878 s	873 sh	874 sh	871 sh	874 s	873 sh
	939 s	939 s	958 vs	939 s	973 vs	939 s	958 vs
ν_2 (H_2O)	—	1631 s	1636 s	1634 s	1635 s	1631 s	1636 s
$\nu_1 + \nu_3$ (H_2O)	3432 w, b	3432 s, b	3439 s, b	3420 s, b	3463 s, b	3440 s, b	3433 s, b
ν (OH)	—	3644 sp	3643 sp	—	3644 sp	3643 sp	3643 sp
ν (CO_3^{2-})	—	1424 s, b	1429 s, b	1428 s	1422 s, b	1420 s, b	1429 s, b
ν (NO_3^-)	—	—	—	1353, 1384 sp	1385 s	—	—

*Band Intensity: vs, very strong; s, strong; sh, shoulder; sp, sharp; b, broad; w, weak.

Table 2
Total metal ions leached after nine (162 h) TCLP extractions

	Ca (wt%) ± 0.5	Si (wt%) ± 0.03	Cr (wt%) ± 0.03
Water/C_3S	38.9	0.35	—
1 *M* Cr(III)/C_3S	42.7	0.35	—
1 *M* Cr(VI)/C_3S	40.3	0.37	1.75

Composition of unleached pastes determined by neutron activation analysis: wt% Ca = 44.3 (± 0.4); wt% Si = 10.7 (±0.43); wt% Cr = 1.8 (±0.05)

In both the one day old Cr(VI) and Cr(III) pastes (Fig. 7(c) and (d)), no significant shift in the SiO_4^{4-} vibrations was observed. In the Cr(VI) paste, a reduced $Ca(OH)_2$ band and another band at 3550 cm^{-1}, possibly due to the lattice water in the calcium chromate hydrate, were observed. The spectra of the Cr(III) doped sample show virtually no $Ca(OH)_2$, corroborating the XRD results discussed earlier (see Fig. 2(c)).

As shown in Fig. 8, after 60 days, substantial amounts of C_3S have reacted in all the samples. In the standard and Cr(VI) pastes, the ν_3 SiO_4^{4-} has only shifted to about 958 cm^{-1} and the ν_4 SiO_4^{4-} has shifted to about 510 cm^{-1}, whereas in the Cr(III) paste, the C_3S reaction is accelerated as demonstrated by the ν_3 SiO_4^{4-} and ν_4 SiO_4^{4-} shifts to 973 cm^{-1} and 489 cm^{-1}, respectively.

A summary of the FTIR spectra assignments is shown in Table 1. Since the Si atoms in the SiO_4^{4-} tetrahedra are displaced in ν_3 and ν_4 vibrational modes, Cr occupying Si sites might also reduce the ν_4 SiO_4^{4-} vibration owing to its higher atomic mass, which would account for the ν_4 SiO_4^{4-} vibration shift to lower wave numbers for the

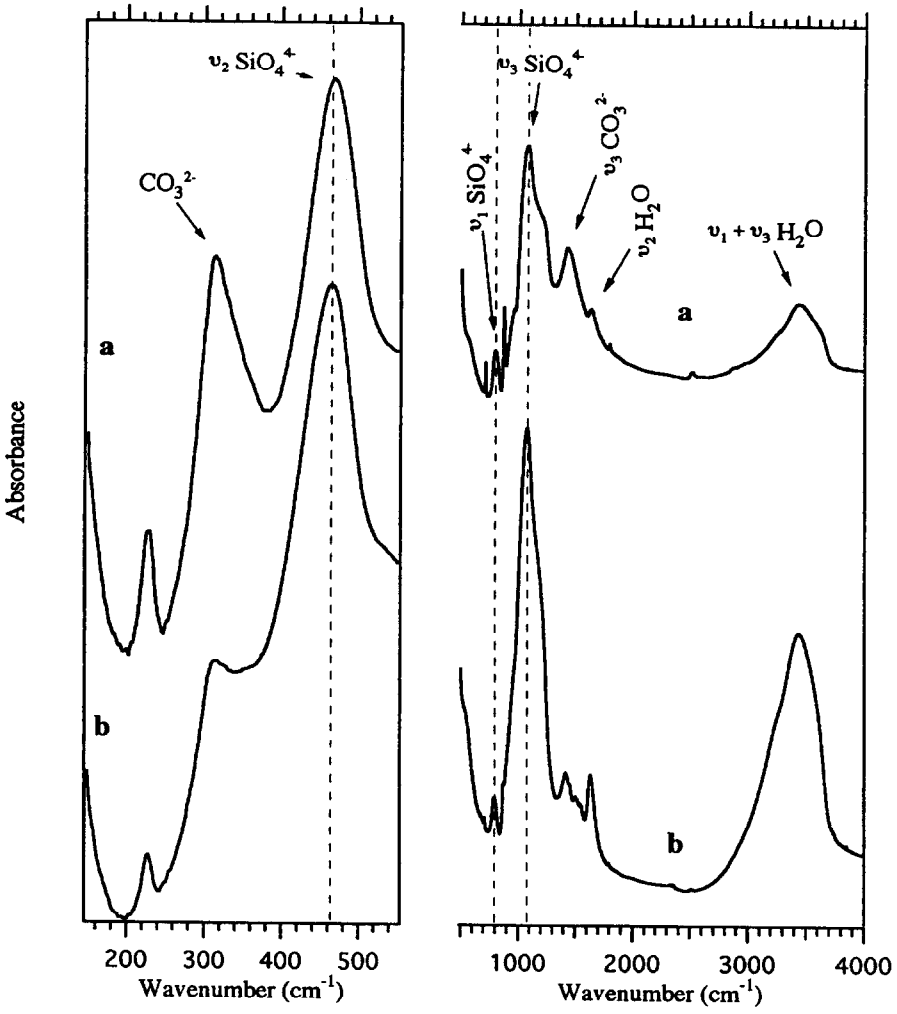

Fig. 9. FTIR (far-IR and mid-IR) of leached samples: (a) H_2O/C_3S; (b) 1 *M* Cr(III)/C_3S.

Cr(III)/C_3S paste. It is evident that there is a larger shift in the v_4 SiO_4^{4-} vibrational mode for the 60 day Cr(III)/C_3S sample (489 cm^{-1}) compared with the 60 day H_2O/C_3S and Cr(VI)/C_3S samples (514 and 513 cm^{-1} respectively). In an aqueous solution, Cr(III) is present as the highly acidic hexaquo cation $(Cr(H_2O)_6)^{3+}$ which can deprotonate to form OH^- bridged polynuclear complexes [16]. As the pH is raised, further deprotonation can occur with the precipitation of hydrated Cr(III) oxide or $Cr(OH)_3$. This dissolves in excess alkali to form $Cr(OH)_4^-$ [16]. $(Cr(OH)_6)^{3-}$ and CrO_4^{2-} may also exist above pH 8 [7].

Silanol groups (≡SiOH) are known to act as ligands in complex formation with transition metals in the same way as water does [17–19]. In a review, Iler [3] noted

Table 3
FTIR (medium-IR and far-IR) spectra assignments of leached Cr-doped tricalcium silicate

Band assignment (cm^{-1})	H_2O/C_3S	$Cr(III)/C_3S$
$\nu_2 + \nu_4$ (SiO_4^{4-})	468 vs	464 vs
ν_1 (SiO_4^{4-})	796 s	796 s
ν_3 (SiO_4^{4-})	1077 vs, b	1077 vs, b
ν_2 (H_2O)	1635 s	1635 s
$\nu_1 + \nu_3$ (H_2O)	3431 b	3440 b
t ($CaCO_3$)	229 s	228 w
t ($CaCO_3$)	313 s	314 w
ν_4 (CO_3^{2-})	713 s	713 w
ν_2 (CO_3^{2-})	873 sp	876 w
ν_3 (CO_3^{2-})	1420 s	1419 s

that SiO_2 suspended in a solution of mostly polyvalent ions, including transition metal ions, begins to adsorb metal ions when the pH is raised to within 1–2 points below the pH at which the metal hydroxide starts to precipitate. The silanol group in the SiO_2 solution gradually replaces the coordinated water. Both mono and bidentate silanol ligands have been observed [19].

Therefore, there is a strong possibility that Cr is contained in the C–S–H during early stages, through ligand substitution of the coordinated water in the hexaquo chromium complex by the silanol species in the pore solution ($H_3SiO_4^-$ and $H_2SiO_4^{2-}$). Measurements of pH within the first few minutes of hydration indicate a pH ~ 6 for the $Cr(III)/C_3S$ paste as opposed to a pH of 11–12 for both the $Cr(VI)/C_3S$ and the standard pastes. The low pH in the Cr(III) doped paste might slow down deprotonation of the hexaquo ion, allowing sufficient time for the silicate anions to displace the coordinated water. As the pH increases, copolymerisation might occur between the silicate anions and $Cr(OH)_4^-$ through a nucleophilic substitution reaction mechanism similar to condensation between two anionic silicate species at pH > 7. An interesting supporting observation was the changing colour of the Cr(III) samples with age. After 24 h, the pastes were green even after removing excess pore solution. The colour changed gradually to grey after 60 days signifying a changing Cr–O environment. The Cr(VI) doped pastes remained yellow throughout the experimental period.

3.3. Leaching studies

The leachate analysis is shown in Table 2. This represents the approximate amounts of Ca, Si and Cr leached from the samples after nine successive acetic acid leaching procedures (TCLP). Virtually no Cr was leached from the 60 day old Cr(III) paste whereas all the Cr was removed in the 60 day old Cr(VI) paste (most of the Cr was leached within the first 18 h). The Ca concentration in the leachates is high due to the dissolution of $Ca(OH)_2$ and some CaO units in the C–S–H. The $CaCO_3$ peaks in the FTIR spectra (Fig. 9) are produced from the reaction between unreacted C_3S and the

acetic acid leaching solution. Increased condensation of the silicate units is evident in the spectra. In all the leached samples, the v_3 SiO_4^{4-} has shifted to 1077 cm^{-1} and the bending vibrations are centered around 460 cm^{-1} with the v_2 and v_4 SiO_4^{4-} overlapping. The band at 798 cm^{-1} was assigned to v_1 SiO_4^{4-}. The silicate structure is close to that of silica gel $(SiO_2)_n \cdot xH_2O$ [20]. The bands at 870 cm^{-1} and 715 cm^{-1} are due to v_2 CO_3^{2-} and v_4 CO_3^{2-} (calcite), respectively. Also the bands at 229 cm^{-1} and 313 cm^1 are due to the translatory lattice modes in calcite. A summary of the band assignments is shown in Table 3.

To completely evaluate the long term stability of waste containment systems, it is essential that the fundamental containment mechanism be understood. Apart from microstructural, microanalytical, molecular and surface characterization of the unleached and leached waste forms, the speciation of the pore solutions should be monitored, particularly during the early stages of hydration reactions.

The results obtained for the C_3S/Cr system studied here do not necessarily translate directly to forms of liquid Cr wastes encountered in real applications. Simple Cr solutions were used in this work to simplify the liquid waste containment system. Future studies are planned to characterize both organic and inorganic Cr complexes typical of actual liquid and solid waste contaminants.

4. Conclusions

This work has confirmed that chromium added as Cr(III) is adequately stabilized/solidified in a C_3S (or OPC) matrix when exposed to an acetic acid leaching solution, but Cr(VI) is not stabilized. It is also observed from the SEM and FTIR results that Cr(III) hinders the formation of fibrous C–S–H and calcium hydroxide in the early stages of hydration reactions. However, in the late stages of hydration, more C–S-H and calcium hydroxide are formed compared to the C_3S/H_2O paste. The SEM/EDS results reveal that Cr is mainly concentrated in the C–S–H areas of the Cr(III) doped samples. Coupled with the infrared studies of the Cr(III) doped samples, which highlight the vibrational shifts in the asymmetric stretch (v_3) and the out-of-plane deformation (v_4), it is apparent that Cr(III) is chemically associated with the silicate polyhedra in the C–S–H and not contained as an insoluble hydroxide or an isolated Cr-complex similar to lead or zinc doped cements [21–23]. As a result of possible ligand substitution and copolymerization between silanol groups and $[Cr(OH)_4]^-$ in the alkaline environment of hydrating C_3S, Cr atoms might occupy Si sites, bonded to the edge or bridging oxygen atoms in the silicate polymeric units.

Acknowledgements

The authors wish to thank the Department of Natural Resources Canada (CANMET), and the Natural Sciences and Engineering Research Council of Canada (NSERC) for providing the financial support for this project.

References

[1] M.E. Gartner and H.M. Jennings, Thermodynamics of calcium silicate hydrates and their solutions, J. Am. Ceram. Soc., 70 (1987) 743–749.

[2] J.D. Ortego, Y. Barroeta, F.K. Cartledge and H. Akhter, Leaching effects on silicate polymerization. An FTIR and ^{29}Si NMR study of lead and zinc in Portland cement, Environ. Sci. Technol., 25 (1991) 1171–1174.

[3] R.K. Iler, The Chemistry of Silica, Wiley, New York, 1979.

[4] R.B. Heimann, D. Conrad, L.Z. Florence, M. Neuwirth, D.G. Ivey, R.J. Mikula and W.W. Lam, Leaching of simulated heavy metal waste stabilized/solidified in different cement matrices, J. Hazard. Mater., 31 (1992) 39–57.

[5] P.L. Bishop, S.B. Ransom and D.L. Gress, Proc. Industrial Waste Conf., Purdue Univ., 1983, pp. 395–401.

[6] D.G. Ivey, R.J. Mikula, W.W. Lam, M. Neuwirth, D.J. Conrad and R.B. Heimann, in: R.D Spence (Ed.), Proc. Chemistry and Microstructure of Solidified Waste Forms, Lewis Publishers, Boca Raton, FL, 1992, pp. 123–149.

[7] M.Y.A. Mollah, Yung-Nien Tsai, T.R. Hess and D.L. Cocke, An FTIR, SEM and EDS investigation of solidification/stabilization of chromium using Portland cement type V and type IP, J. Hazard. Mater., 30 (1992) 273–283.

[8] L.G. Butler, F.K. Cartledge, H.C. Eaton and M.E. Tittlebaum, in: R.D. Spence (Ed.), Chemistry and Microstructure of Solidified Waste Forms, Lewis Publishers, Boca Raton, FL, 1992, 151–167.

[9] E.E. Pressler, S. Brunauer, D.L. Kantro and C.H. Weise, Determination of the free hydroxide contents of hydrated Portland cements and calcium silicates, Anal. Chem., 33 (1961) 877–882.

[10] US Environmental Protection Agency Federal Register, 51, 1986, pp. 21685–21688.

[11] E.M. Larsen, Transitional Elements, W.A Benjamin, New York, 1965, p. 110.

[12] S.N. Ghosh and A.K. Chatterjee, Absorption and reflection infrared spectra of major cement minerals, clinkers and cements, J. Mater. Sci., 9 (1974) 1577–1584.

[13] J. Bensted and S.P. Varma, Some applications of infrared and Raman spectroscopy in cement industry, Part 2 – Portland cement and its constituents, Cem. Technol., 5 (1974) 378–382.

[14] M. Handke and M.E. Jurkiewicz, IR and Raman spectroscopy studies of tricalcium silicate structure, Ann. Chim. Fr., 4 (1979) 145–161.

[15] K. Nakamoto, Infrared and Raman Spectra of Inorganic and Coordination Compounds, 4th edn., Wiley, New York, 1986, p. 228.

[16] N.N. Greenwood and A. Earnshaw, Chemistry of the Elements, Pergamon, New York, 1984, pp. 1190–1199.

[17] R.O. James and T.W. Healy, Adsorption of hydrolyzable metal ions at the oxide–water interface, III. A thermodynamic model of adsorption, J. Colloid Interface Sci., 40 (1972) 65–81.

[18] L.L. Olsen and C.R. O'melia, The interaction of Fe(III) with $Si(OH)_4$, J. Inorg. Nucl. Chem., 35 (1973) 1977–1985.

[19] P.W. Schindler, B. Furst, R. Dick and P.U. Wolf, Ligand properties of surface silanol groups, I. Surface complex formation with Fe^{3+}, Cu^{2+}, Cd^{2+} and Pb^{2+}, J. Colloid Interface Sci., 55 (1976) 469-475.

[20] R.A. Nyquist, Infrared Spectra of Inorganic Compounds (3800-45 cm^{-1}), Academic Press, New York, 1971, p. 94.

[21] F.K. Cartledge, L.G. Butler, D. Chalasani, H.C. Eaton, F.P. Frey, E. Herrera, M.E. Tittlebaum and Yang, Shou-Lan, Immobilization mechanisms in solidification/stabilization of Cd and Pb salts using Portland cement fixing agents, Environ. Sci. Technol., 24 (1990) 867–873.

[22] C.S. Poon, A.I. Clark, C.J. Peters and R. Perry, Mechanisms of metal fixation and leaching by cement based fixation processes, Waste Manag. Res., 3 (1985) 127–142.

[23] I. Jawed, J. Skanly and J.F. Young, in: P. Barnes (Ed.), Structure and Performance of Cement, Applied Science Publishers, Barking, 1983, p. 259.